Bioorganic Chemistry 83 (2019) 105–110

Contents lists available at ScienceDirect

Bioorganic Chemistry

journal homepage: www.elsevier.com/locate/bioorg

Trichosanhemiketal A and B: Two 13,14-*seco*-13,14-epoxyporiferastanes from the root of *Trichosanthes kirilowii* Maxim.

Manh Tuan Ha[a,b], Thanh Nam Phan[c], Jeong Ah Kim[d,*], Won Keun Oh[e], Jeong Hyung Lee[c], Mi Hee Woo[a], Byung Sun Min[a,*]

[a] College of Pharmacy, Drug Research and Development Center, Daegu Catholic University, Gyeongbuk 38430, Republic of Korea
[b] Laboratory of Research and Applied Biochemistry, Center for Research and Technology Transfer, Vietnam Academy of Science and Technology, Hanoi, Viet Nam
[c] College of Natural Science, Kangwon National University, Kangwon 200-701, Republic of Korea
[d] College of Pharmacy, Research Institute of Pharmaceutical Sciences, Kyungpook National University, Daegu 41566, Republic of Korea
[e] College of Pharmacy, Seoul National Univeristy, Seoul 08826, Republic of Korea

ARTICLE INFO

Keywords:
Trichosanthes kirilowii
Cucurbitaceae
Trichosanhemiketal
Anti-inflammation
NO production

ABSTRACT

Of the 32 *Trichosanthes* species in China, *T. kirilowii* Maxim. is the most renowned species used in traditional Chinese medicine and has diverse pharmacological properties. However, most of the phytochemical studies of *T. kirilowii* have focused on the fruits and seeds. In our investigation of the chemical constituents of *T. kirilowii* roots, two previously undescribed sterols [trichosanhemiketal A and B (**1** and **2**)], together with 13 known compounds, were isolated and their structures were elucidated. To the best of our knowledge, this represents the first isolation of compounds with a 13,14-*seco*-13,14-epoxyporiferastane (**1**–**2**) skeleton from the Cucurbitaceae family. The anti-inflammatory activity of the isolated compounds was determined through an analysis of their inhibitory effects on lipopolysaccharide (LPS)-induced nitric oxide (NO) production in macrophage RAW264.7 cells. Of the compounds, **4**, **5**, **6**, and **8** showed significant inhibitory activities, with IC_{50} values of 8.5, 15.1, 25.4, and 28.5 μM, respectively. In addition, compound **4** inhibited inducible nitric oxide synthase (iNOS) and cyclooxygenase (COX)-2 expression in a concentration-dependent manner.

1. Introduction

The Cucurbitaceae family is a moderately large family of approximately 130 genera and 900 species [1]. From a botanical perspective, this family can be divided into two sub-families: the Cucurbitoideae and the Zanonioideae [2]. Most are abundant within the tropics, especially in tropical Africa and the neotropics [1]. The plants from these families are predominantly cultivated as vegetables; various parts of the plant are used, including the seeds, flowers, very young shoots with tendrils, and roots, but mainly the fruits. Other uses, including medicinal use, have been recorded [2].

The genus *Trichosanthes* (Cucurbitaceae), belonging to the tribe Trichosantheae of the sub-family Cucurbitoideae, consists of approximately 100 species distributed from eastern Asia to tropical Australia and Fiji [1,3]. It is the largest genus in the family and has emerged as a considerable resource for the discovery of anticancer drugs [4]. Diverse pharmacological properties have been reported for some species of this genus, including *T. kirilowii, T. dioica*, and *T. cucumerina,* which have promising antihyperglycemic, antihyperlipidemic, antitumor, cytotoxic, anti-inflammatory, antidiarrheal, antiosteoarthritic, and antifungal activities and also ameliorate arsenic poisoning [4–7]. There are approximately 32 *Trichosanthes* species in China, of which *T. kirilowii* Maxim. is the most renowned species in traditional Chinese medicine and has been the focus of medicinal investigations [4]. All parts of *T. kirilowii* can serve as herbal medicinal products. In traditional Chinese medicine, the seeds and roots of *T. kirilowii* are used for the treatment of inflammation, cough, phlegm, polydipsia, and diabetes [8,9]; whereas the tuber has been used as an abortifacient for over 1000 years because of its extreme toxicity to trophoblasts [10]. Most phytochemical studies of *T. kirilowii* have focused on the fruits and seeds, from which fatty acids, volatile oils, triterpenoids, triterpenoid cucurbitacins, sterols, flavones, and microelements have been isolated [10–14]. In particular, trichosanthin, the well-known type I ribosome-inactivating protein purified from the root tuber of *T. kirilowii*, exhibits a wide spectrum of medicinal activities, including antitumor, anti-HIV, and immunoregulatory functions [15]. To conduct further investigations into the chemical composition of *T. kirilowii* root, which has rarely been addressed, a systematic investigation was performed. As a result,

* Corresponding authors.
E-mail addresses: jkim6923@knu.ac.kr (J.A. Kim), bsmin@cu.ac.kr (B.S. Min).

https://doi.org/10.1016/j.bioorg.2018.10.019
Received 19 July 2018; Received in revised form 9 October 2018; Accepted 9 October 2018
Available online 13 October 2018

two previously undescribed sterols (13,14-*seco*-13,14-epoxyporiferastanes), together with 13 known compounds, were obtained from the methanol extract. The anti-inflammatory activity of the isolated compounds was examined for their inhibitory effects on lipopolysaccharide (LPS)-induced nitric oxide (NO) production in RAW264.7 macrophages. To the best of our knowledge, this represents the first isolation of compounds with the 13,14-*seco*-13,14-epoxyporiferastane skeleton from the Cucurbitaceae family.

2. Experimental section

2.1. General experimental procedures

The optical rotations were measured using a Jasco P-1020 polarimeter. The IR spectra were recorded using a Bruker IFS-66/S Fourier transform (FT)-IR spectrometer. The UV spectra were recorded using an Agilent 8453 UV–visible spectrophotometer. The HR-ESI-MS spectra were recorded using a Micromass QTOF2-MS mass spectrometer. The NMR spectra were recorded using Bruker 500 MHz, 700 MHz, and 900 MHz spectrometers and a Varian Unity Inova 400 MHz spectrometer using TMS as the internal standard. The packing material for the molecular sieve CC was Sephadex LH-20 (Pharmacia Company). Silica gel 60 (Merck, 230–400 mesh) and reversed phase (RP)-C_{18} silica gel (Merck, 75 mesh) were used for column chromatography (CC). TLC was performed using Merck precoated silica gel F_{254} plates and RP-18 F_{254s} plates, and compounds were visualized by spraying with aqueous 10% H_2SO_4 and heating for 3–5 min. Preparative HPLC was performed using a Waters Alliance 2695 HPLC system with a Waters 2996 photodiode array detector, and an YMC-Pack ODS-A column (25 × 250 mm, 5 μm particle size, YMC Co. Ltd, Japan). The conformation search was performed with Conflex 7 (Conflex Corp., Tokyo, Japan). The geometrical optimization of the computed conformers was carried out and visualized with TmoleX 3.4 and Turbomole (COSMOLogic GmbH, Leverkusen, Germany).

2.2. Chemicals and reagents

Solvents were purchased from Samchun Chemicals Co. Korea. RPMI 1640, fetal bovine serum (FBS), phosphate buffered saline (PBS) buffer, penicillin–streptomycin were purchased from Gibco (Carlsbad, CA, U.S.A.). MTT (3-(4,5-dimethylthiazol-2-yl)-2,5-diphenyltetrazolium bromide) reagent and dimethyl sulfoxide (DMSO) were obtained from Sigma Aldrich.

2.3. Plant material

The root of *T. kirilowii* was from purchased DaeMyung Pharm. Co. Ltd. (Lot. No. 018-170407), Republic of Korea and authenticated by Prof. Byung-Sun Min, College of Pharmacy, Daegu Catholic University, Republic of Korea. The voucher specimen CUD-2870-1 was deposited at the Herbarium of the College of Pharmacy, Daegu Catholic University, Republic of Korea.

2.4. Extraction and isolation

The root of *T. kirilowii* (3.0 kg) was extracted with MeOH (4 × 5 L) under reflux and then filtered. The MeOH solution was concentrated under reduced pressure to produce a residue (550 g), which was suspended in distilled water (H_2O) and then successively partitioned with *n*-hexane and *n*-butanol to afford *n*-hexane (59 g) and *n*-butanol (40 g) fractions, and an H_2O layer. The *n*-hexane fraction (59 g) was further fractionated by column chromatography with silica gel and eluted by a gradient of 0–100% acetone in CH_2Cl_2 (v/v) to yield 20 fractions (H1–H20). Fraction H18 (452 mg) was chromatographed on a reversed-phase C_{18} (RP-C_{18}) silica gel column using the MeOH-H_2O solvent system (3:1, v/v) to produce five sub-fractions (H18.1-H18.5). Sub-fraction H18.3 (35.5 mg) was separated by using preparative RP-HPLC [Waters Alliance 2695 HPLC system; YMC-Pack ODS-A column (25 × 250 mm, 5 μm particle size; UV detection at 254 nm] with an isocratic solvent system [85% MeOH in H_2O (v/v)] in a 0.05% Trifluoroacetic acid (TFA) at a flow rate of 5 mL/min as the mobile phase to yield **1** (4.0 mg, t_R = 29.4 min) and **2** (2.0 mg, t_R = 37.3 min). Fraction H17 (525 mg) was fractionated on a silica gel column using CH_2Cl_2-EtOAc (10:1, v/v) as the mobile phase to yield nine sub-fractions (H17.1-H17.9). Sub-fraction H17.7 (45.5 mg) was passed over a silica gel column eluted by CH_2Cl_2-acetone (12:1, v/v) to afford **14** (7.2 mg). By using a similar procedure as that described for sub-fraction H17.7, compound **15** (4.5 mg) was produced from sub-fraction H17.9 (55.6 mg). Compound **9** (130.5 mg) was purified from fraction H8 (456.7 mg) on a silica gel column by using a mobile phase of CH_2Cl_2–MeOH (30:1, v/v). The *n*-butanol (40 g) fraction was fractionated on a silica gel column and eluted by a gradient of 0–100% MeOH in CH_2Cl_2 (v/v) to afford 14 fractions (B1–B14). Fraction B5 (520.5 mg) was separated on an RP-C_{18} silica gel column by using the MeOH-H_2O solvent system (2.5:1, v/v) to yield **8** (3.5 mg), **3** (10.0 mg), and **4** (12.4 mg). Compounds **5** (8.5 mg) and **6** (11.0 mg) were obtained from fraction B7 (434.5 mg) by column chromatography, using an RP-C_{18} silica gel column and a CH_3CN-H_2O solvent system (1.5:1, v/v). Through the same process, fraction B10 (414.0 mg) yielded **11** (4.0 mg) and **13** (5.4 mg). Fraction B4 (215.5 mg) was separated on a silica gel column by using CH_2Cl_2–MeOH (10:1, v/v) as the mobile phase to yield **7** (4.5 mg) and **12** (4.0 mg). Compound **10** (2.0 mg) was purified from fraction B13 (156.5 mg) on an RP-C_{18} silica gel column using a mobile phase of MeOH–H_2O solvent system (3:1, v/v).

2.4.1. Trichosanhemiketal A (*1*)

Colorless oil; $[\alpha]_D^{21}$ +30.5 (*c* 0.065, $CHCl_3$); IR (KBr) ν_{max} 3447, 3019, 1706, 1647, 1508, 1033 cm^{-1}; UV (MeOH) λ_{max} (log ε) 248 (2.18) nm; ECD (*c* 0.0021 mM, $CHCl_3$): $\Delta\varepsilon_{299}$ +0.30, $\Delta\varepsilon_{248}$ +2.05, $\Delta\varepsilon_{221}$ +0.64 (observed as a valley), $\Delta\varepsilon_{204}$ +2.03; ^1H (700 MHz in $CDCl_3$) and ^{13}C NMR (175 MHz in $CDCl_3$) data, see Table 1; HR-ESI-MS *m/z* 481.3291 ($[M+Na]^+$, calcd for 481.3294) and *m/z* 459.3460 ($[M+H]^+$, calcd for 459.3474).

2.4.2. Trichosanhemiketal B (*2*)

Colorless oil; $[\alpha]_D^{21}$ +25.6 (*c* 0.051, $CHCl_3$); IR (KBr) ν_{max} 3448, 3019, 1706, 1646, 1508, 1033 cm^{-1}; UV (MeOH) λ_{max} (log ε) 247 (1.44) nm; ECD (*c* 0.0021 mM, $CHCl_3$): $\Delta\varepsilon_{303}$ +0.71, $\Delta\varepsilon_{250}$ +1.69, $\Delta\varepsilon_{224}$ +1.10 (observed as a valley), $\Delta\varepsilon_{209}$ +2.54; ^1H (900 MHz in $CDCl_3$) and ^{13}C NMR (225 MHz in $CDCl_3$) data, see Table 1; HR-ESI-MS *m/z* 461.3621 ($[M+H]^+$, calcd 461.3631) and *m/z* 483.3448 [$M+Na]^+$ (calcd 483.3450).

2.5. Computational methods for ECD calculations

The calculated electronic circular dichroism (ECD) spectra of **1** and its enantiomer were performed according to the previously published protocol [16]. Conformational searches were performed using MMFF94s force-field calculations with an energy cutoff of 10.0 kcal/mol in Conflex 7 (Conflex Corp., Tokyo, Japan). Among the generated conformers, ten conformers were selected, the sum of their expected population was above 75%. These selected conformers were optimized by density functional theory (DFT) calculations at the B3LYP/def-SV(P) level in the gas phase, using TmoleX 3.4 and Turbomole (COSMOLogic GmbH, Leverkusen, Germany). After optimization, the ECD spectra of the optimized conformers were calculated using time-dependent DFT (TDDFT) at the B3LYP/6-31G level.

2.6. Cell culture

RAW264.7 cells were purchased from the American Type Culture Collection (Manassas, VA, USA) and were maintained in Dulbecco's modified essential medium supplemented with penicillin (100 units/

Table 1
^{1}H and ^{13}C NMR spectroscopic data for compounds 1 and **2** in $CDCl_3$.

Position	1		2	
	δ_H[a] mult., (*J* in Hz)	δ_C[b]	δ_H[c] mult., (*J* in Hz)	δ_C[d]
1α	1.35, m	34.3	1.36, m	34.5
1β	2.05, m		1.36, m	
2α	1.96, m	31.4	1.96, m	31.5
2β	1.57, m		1.56, m	
3	3.66, tt, (10.5, 4.9)	70.1	3.66, tt, (10.8, 4.5)	70.1
4α	1.71, m	37.0	1.72, m	37.1
4β	1.38, m		1.39, m	
5	1.86, m	39.5	1.88, m	39.6
6α	2.24, dd (18.2, 4.2)	41.4	2.26, dd (18.9, 4.5)	41.5
6β	2.30, m		2.30, m	
7		201.3		201.5
8		135.7		136.2
9		172.4		172.8
10		40.2		40.2
11α	2.29, m	21.7	2.30, m	21.9
11β	2.92, t (11.9)		2.88, m	
12	1.71, m	41.0	1.71, m	41.7
	1.76, m		1.75, m	
13		76.5		76.3
14		99.3		99.1
15	1.68, m	33.7	1.84, m	32.5
	1.77, m		1.85, m	
16	1.53, m	20.3	1.56, m	17.6
	1.70, m		1.75, m	
17	1.04, m	45.2	1.07, m	45.3
18	1.29, s	28.2	1.24, s	26.9
19	1.05, s	15.5	1.06, s	15.9
20	2.61, dd (14.0, 6.3)	35.9	1.80, m	33.9
21	1.07, d (6.3)	23.3	0.95, d (6.3)	20.3
22	5.39, dd (15.4, 8.4)	130.6	1.80, m	35.5
			1.85, m	
23	5.13, dd (15.4, 9.1)	136.4	1.14, m	29.3
			1.20, m	
24	1.60, m	51.6	0.99, m	45.9
25	1.53, m	32.1	1.67, m	29.2
26	0.76, d (6.3)	19.2	0.79, d (6.3)	19.2
27	0.80, d (6.3)	21.2	0.81, d (6.3)	19.9
28	1.19, m	25.6	1.21, m	23.4
	1.40, m		1.27, m	
29	0.79, t (7.0)	12.6	0.83, t (7.2)	12.3

[a] NMR data were measured in $CDCl_3$ at 700 MHz.
[b] NMR data were measured in $CDCl_3$ at 175 MHz.
[c] NMR data were measured in $CDCl_3$ at 900 MHz.
[d] NMR data were measured in $CDCl_3$ at 225 MHz.

mL)-streptomycin (100 mg/mL) and 10% heat-inactivated fetal bovine serum (Cambrex, Charles City, IA, USA). The cells were maintained in a humidified atmosphere with 5% CO_2 at 37 °C.

2.7. Measurement of NO and cell viability assay

RAW264.7 cells were seeded in 24-well plates at a density 5×10^5 cells/well. The plates were pretreated with various concentrations of the test compounds for 30 min and then incubated for another 24 h with or without 1 μg/mL of lipopolysaccharide (LPS). Nitrite concentration in the culture supernatant was measured by the Griess reaction. The nitrite level in each sample was calculated through comparison with a standard curve generated with sodium nitrite. Cell viability was measured by using an MTT [3-(4,5-dimethylthiazolyl-2)-2,5-diphenyltetrazolium bromide]-based colorimetric assay. The reduction of MTT to formazan within the cells was quantified by measuring OD_{570} [17].

2.8. Western blotting analysis

Western blot analysis was performed in accordance with our previously described protocol [18]. Briefly, cells were lysed in lysis buffer [50 mM Tris-HCl (pH 7.4), 150 mM NaCl, 1 mM EDTA, 5 mM sodium orthovanadate, 1% NP-40, and protease inhibitors cocktail (BD Biosciences, New Jersey, USA)]. In experiments, the cytoplasmic and nuclear fractions were prepared by using NE-PER Nuclear and Cytoplasmic Extraction Reagent Kit (Thermo Fisher Scientific, Rockford, IL, USA). A total of 50 μg of protein per lane was resolved by using sodium dodecyl sulfate-polyacrylamide gel electrophoresis, transferred to a polyvinylidene difluoride membrane, and probed with the appropriate antibodies. The signal was detected using an enhanced chemiluminescent system (Intron, Seongnam, Korea).

2.9. Statistical analysis

Statistical analyses were performed by one-way analysis of variance (ANOVA), followed by the Fisher least significant difference test. $P < 0.05$ was considered statistically significant. The results are presented as the mean ± standard error of mean (SEM).

3. Results and discussion

3.1. Structure determination of isolated compounds

The methanolic extract of the dry roots of *T. kirilowii* was partitioned sequentially in *n*-hexane, *n*-butanol, and water. Repeated column chromatography (silica gel, RP-18) of the *n*-hexane and *n*-butanol fractions led to the isolation of 15 compounds (**1–15**) (Fig. 1).

Trichosanhemiketal A (**1**) was isolated as a colorless oil with positive optical rotation. The molecular formula of **1** was determined to be $C_{29}H_{46}O_4$ by HRESI-MS with a sodium adduct molecular ion peak at *m/z* 481.3291 ($[M+Na]^+$, calcd for 481.3294) and a protonated molecular ion peak at *m/z* 459.3460 ($[M+H]^+$, calcd for 459.3474), which implied seven degrees of unsaturation. The UV spectrum exhibited an absorption maximum at 248 nm. The presence of hydroxy and carbonyl groups was indicated by the IR absorption at 3447 and 1706 cm^{-1}, respectively. The ^{1}H NMR spectrum of **1** exhibited characteristic resonances of one primary methyl at δ_H 0.79 (t, $J = 7.0$, H-29); three secondary methyls at δ_H 0.76 (H-26), 0.80 (H-27), and 1.07 (H-21); two tertiary methyls at δ_H 1.05 (H-19) and 1.29 (H-18); one oxygen-bearing methine at δ_H 3.66 (tt, $J = 10.5$, 4.9, H-3); and a disubstituted olefin at δ_H 5.39 (dd, $J = 15.4$, 8.4, H-22) and 5.13 (dd, $J = 15.4$, 9.1, H-23) (Table 1). The ^{13}C NMR and DEPT spectra of **1** (Table 1) revealed 29 signals, including six methyls, nine methylenes, two sp^2 and six sp^3 methines, and three sp^2 and three sp^3 quaternary carbons. The three degrees of unsaturation for the formula were attributed to two sets of olefinic groups at δ_C 130.6 (C-22), 136.4 (C-23), 135.7 (C-8), 172.4 (C-9), and an unsaturated ketone carbonyl carbon at δ_C 201.3. The remaining degrees of unsaturation were therefore attributed to the presence of four rings. The ^{1}H–^{1}H COSY correlations of H_2-15–H_2-16–H-17–H-20, H_3-21–H-20–H-22–H-23–H-24–H_2-28–H_3-29, and H_3-26–H-25–H_3-27, together with the HMBC correlations from H_3-21 to C-17/C-22 and from H-20 to C-13/C-17/C-16, suggested that the side chain was a typical poriferast-24-ethyl-Δ^{22}-type structure (Figs. 1 and 2) [13]. The location of the ketone carbonyl carbon C-7 was confirmed by the HMBC correlations between H-5/H_2-6 and C-7. In addition, the HMBC correlations from H_3-19/H_2-11/H_2-12 to C-9 and from H_2-6/H_2-11 to C-8 indicated the olefinic group at δ_C 135.7 and 172.4 was attributed to C-8 and C-9 (Fig. 2). Except for the four quaternary carbons at C-7, 8, 9, 10, the remaining quaternary carbons, including one oxygenated carbon (δ_C 76.5) and one hemiketal carbon (δ_C 99.3), were assigned to C-13 and C-14, respectively [19,20]. This indicated that an epoxy-bridge was formed between C-13 and C-14, replacing the carbon-carbon linkage. This was confirmed by the HMBC correlations between H-20/H_3-18/H_2-11/H_2-12/H_2-15 and C-13 and between H_3-18/H_2-15/H_2-16 and C-14 (Fig. 2). In addition, evidence for the 3β-hydroxyl-cyclohexanol structure (ring A) of **1** was provided by the COSY correlations of H_2-1–H_2-2–H-3–H_2-4–H-5, and the coupling constants of H-3 (tt, $J = 10.5$, 4.9)

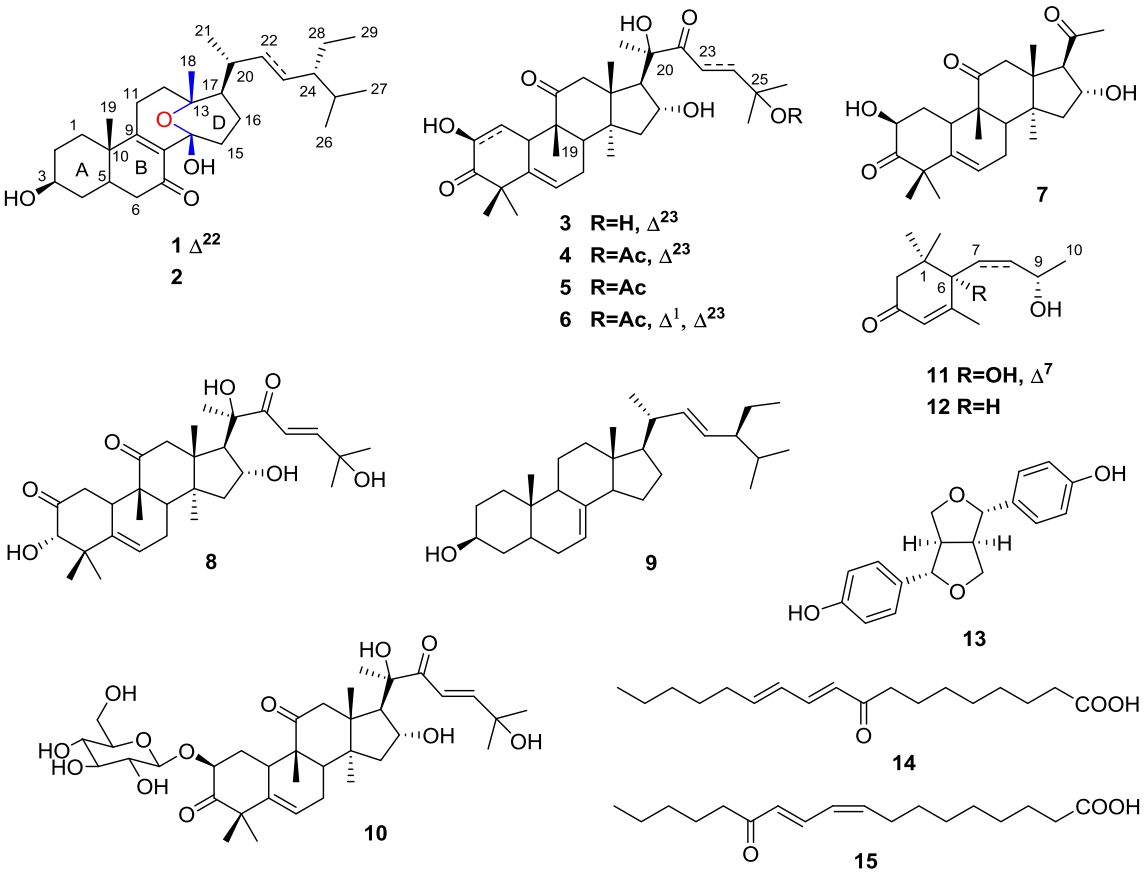

Fig. 1. Chemical structures of compounds **1–15**.

(Fig. 2). A careful comparison of the NMR data of **1** with those of eringiacetal B revealed their structural similarities with regard to the 3*β*-hydroxyl-13,14-*seco*-13,14-epoxyergostane-8,22-dien-7-one structure [19]. The differences were the 24-ethylporiferastane side chain and the absence of the olefinic group at C-5/C-6 in **1**. Assignments of all ^{1}H and ^{13}C NMR signals were accomplished by interpretation of HSQC and HMBC spectra (Fig. 2).

The stereochemistry of the unsaturated side chain was established as (22*E*, 24*R*) based on the coupling constants [H-22 (dd, J = 15.4, 8.4), H-23 (dd, J = 15.4, 9.1)] and comparison with the literature data of similar structures [13,21,22]. The ROESY correlation from H-5 (δ_H 1.86) to H-3 (δ_H 3.66) revealed that H-5 and H-3 were cofacial and *α*-oriented (Fig. 2). To stabilize this structure without distortion, the relative configuration of the C and D rings was deduced to be *cis*, which meant that C-13 and C-14 were oriented in the same direction and Me-18–C-13–O–C–14-14-OH adopted the W-type conformation [19]. In addition, Bjelaković et al. demonstrated that two types of stereochemistry, such as (13*R*, 14*S*) and (13*S*, 14*R*), cannot co-exist stably owing to strain [23]. Therefore, the stereochemistry at C-13 and C-14 could only be (*R*, *R*) or (*S*, *S*). Moreover, the ROESY cross-peaks between H_3-19 (δ 1.05)/H-20 (δ_H 2.61)/H-11β (δ_H 2.92) and H_3-18 (δ 1.29), as well as between H-11α (δ_H 2.29) and H-17 (δ 1.04), indicated

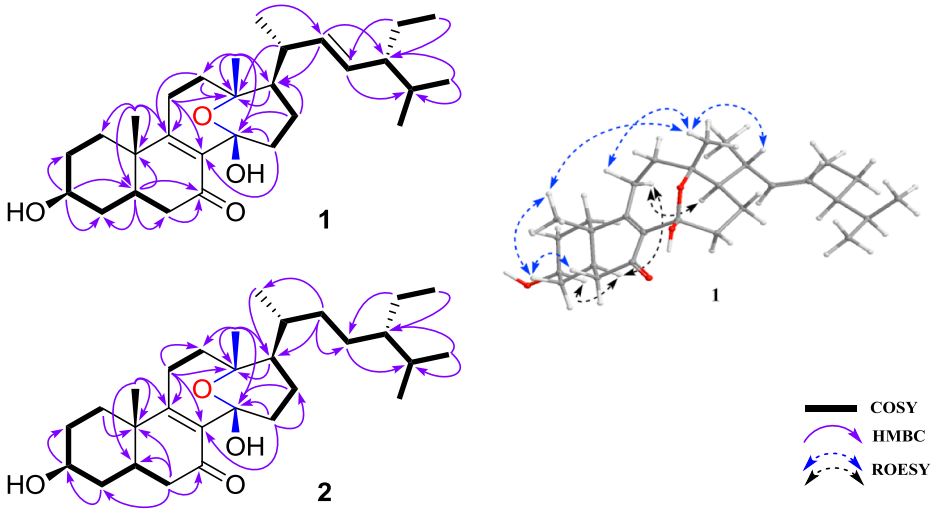

Fig. 2. Key COSY, HMBC, and ROESY correlations of compounds **1** and **2**.

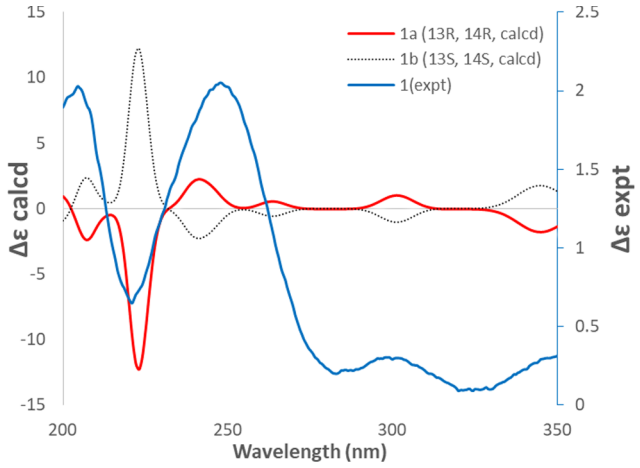

Fig. 3. Experimental and calculated ECD spectra for **1**.

that Me-18 was *β*-oriented (Fig. 2). Thus, the 14-OH group was also on the same side, with *β*-direction. In addition, **1** displayed positive optical rotation, which was similar to that of eringiacetal B (13,14-*seco*-13,14-epoxyergostane-5,8,22-trien-7one) [19]. Therefore, the stereochemistry of **1** at C-13 and C-14 was elucidated as (*R*, *R*) [19]. To further confirm the absolute configuration of **1**, the calculated electronic circular dichroism (ECD) spectra for the 13,14-*seco*-13,14-epoxyporiferastane structure was performed for the first time. The absolute configurations of the stereogenic centers C-13 and C-14 of **1** were established by theoretical calculations of its ECD using the time-dependent density functional theory (TDDFT) method at the B3LYP/6-31G level. The results showed that the calculated CD spectrum of the 13*R*, 14*R* configurations displayed consistency with the experimental CD spectrum of **1**, whereas the enantiomer (13*S*, 14*S*) showed a contrasting profile (Fig. 3). Therefore, the stereochemistry of **1** was confirmed as (13*R*, 14*R*). Based on the above analysis, the structure of **1** was determined as 3*β*-hydroxyl-13,14-*seco*-13*R*,14*R*-epoxyporiferastane-8,22-dien-7-one (Fig. 1), a previously undescribed steroid, which we named as trichosanhemiketal A.

Trichosanhemiketal B (**2**) was also obtained as a colorless oil and had the molecular formula $C_{29}H_{48}O_4$, which was identified by HRESI-MS with a protonated molecular ion peak at *m/z* 461.3621 $[M+H]^+$ (calcd 461.3631) and a sodium adduct molecular ion peak at *m/z* 483.3448 $[M+Na]^+$ (calcd 483.3450), with two more hydrogen atoms than that in **1**. The IR and UV spectra of **2** were similar to those of **1**. The ^1H, ^{13}C NMR, and DEPT spectra revealed the presence of one primary methyl [δ_H/δ_C 0.83 (t, J = 7.2, H-29)/12.3], three secondary methyls [δ_H/δ_C 0.79 (d, J = 6.3, H-26)/19.2, 0.81 (d, J = 6.3, H-27)/19.9, and 0.95 (d, J = 6.3, H-21)/20.3]; two tertiary methyls [δ_H/δ_C 1.06 (s, H-19)/15.9, 1.24 (s, H-18)], one oxygenated methine [δ_H/δ_C 3.66 (tt, J = 4.5, 10.8, H-3)/70.1], one double bond [δ_C 136.2 172.8]; and one ketone [δ_C 201.5]. All the above structural features for **2** closely resembled with those of **1**, except for the absence of double bonds (Δ^{22}) in **2**, which suggested that **2** was the 22,23-dihydride of **1**. This was confirmed by the HSQC, HMBC, and ^1H-^1H COSY experiments (Fig. 2). The stereochemistry of the saturated side chain was established as (24β/*S*) by the comparison with the literature data of similar sterols [13,21,22]. In addition, **1** and **2** had similar ECD data (see Figs. S1.9 and S2.9, Supporting data) and positive optical rotations, which suggested that they have the same stereochemistry at C-13 and C-14. Thus, the structure of **2** was determined as 3*β*-hydroxyl-13,14-*seco*-13,14-epoxyporiferastane-8-en-7-one (Fig. 1), a previously undescribed steroid, and named trichosanhemiketal B.

On the basis of comprehensive analysis of spectroscopic data and comparison with literature, the chemical structures of the 13 known compounds were identified as cucurbitacins D (**3**), B (**4**), E (**6**) [24], 23,24-dihydrocucurbitacin B (**5**) [25,26], hexanorcucurbitacin D (**7**) [27], isocucurbitacin D (**8**) [28], spinasterol (**9**) [11], arvenin III (**10**) [29], blumenol A (**11**) [30], C (**12**) [31], ligballinol (**13**) [32], (10*E*,12*E*)-9-oxo-10,12-octadecadienoic acid (**14**) [33], and (9*Z*,11*E*)-13-oxo-9,11-octadecadienoic acid (**15**) [33] (Fig. 1).

Table 2
Inhibitory effect of isolated compounds on nitric oxide production in RAW264.7 cells.

Compounds	IC_{50} (μM)[a]
1	> 30
2	> 30
3	> 30
4	8.5 ± 1.2
5	15.1 ± 1.3
6	25.4 ± 3.4
7	> 30
8	28.5 ± 2.5
9	> 30
10	> 30
11	–
12	–
13	–
14	–
15	–
Celastrol[b]	1.15 ± 0.87

[a] The inhibitory effects are represented as the molar concentration (μM) giving 50% inhibition (IC_{50}) relative to the vehicle control. These data represent the average values of three repeated experiments.
[b] Positive control for NO production. (-) No test.

3.2. Anti-inflammatory activity of isolated compounds

To assess the anti-inflammatory effects of the isolated compounds from the root of *T. kirilowii*, we investigated whether the compounds inhibited NO production in LPS-stimulated RAW264.7 cells. These cells were stimulated with 1 μg/mL LPS for 24 h in the presence of compounds **1–10**, and the levels of NO in the culture supernatants were measured using Griess reaction. No levels were increased in RAW264.7 untreated cells stimulated with LPS; however, pretreatment of cells with compounds **4**, **5**, **6**, and **8** led to attenuated NO production in a concentration-dependent manner, with IC_{50} values of 8.5, 15.1, 25.4, and 28.5 μM, respectively; compared with the positive control, celastrol (IC_{50} = 1.15 μM) (Table 2). The other compounds (**1**, **2**, **3**, **7**, **9**, **10**) did not show any considerable inhibitions of NO and displayed weak IC_{50} values (≥ 30 μM). In addition, the tested compounds did not affect cell viability at the range of concentrations (1–30 μM) that inhibited the LPS-induced inflammatory response, as measured by an MTT assay (data not shown).

We next assessed whether the most active compound (**4**) suppressed the expression of inducible NO synthase (iNOS) and cyclooxygenase-2 (COX-2) in LPS-stimulated RAW264.7 cells. The cells were stimulated with LPS in the presence of these compounds at various concentrations (0.3–10 μM), and iNOS and COX-2 expression was determined by Western blot analysis. The results indicated that cucurbitacin B (**4**) exhibited significant inhibition of LPS-induced iNOS expression in a concentration-dependent manner (Fig. 4). In a previous study, eringiacetal B (13,14-*seco*-13,14-epoxyergostane-5,8-dien-7-one) was found to inhibit NO production with an IC_{50} of 13.0 μM [19]. Unfortunately, trichosanhemiketals A and B (**1**, **2**) [13,14-*seco*-13,14-epoxyporiferastane-8-en-7-one derivatives] exerted only a weak inhibitory activity on the production of NO ($IC_{50} \geq 30$ μM), which suggested that the appearance of double bond ($\Delta^{5,6}$) and the 24-methyl group in eringiacetal B may have a positive influence on this activity.

Similar structure-activity relationships were observed in the NO assay for the cucurbitacins (**4–6**). The 25-$OCOCH_3$ cucurbitacins (**4**, **5**,

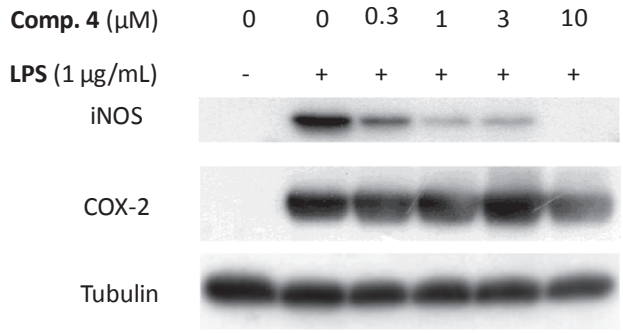

Fig. 4. Inhibition of LPS-Induced iNOS and COX-2 expression in RAW264.7 cells by **4**. RAW264.7 cells were pretreated for 30 min indicated concentrations (0.3–10 μM) of **4**, followed by stimulation with LPS (1 μg/mL) for 18 h. Total lysates were prepared, the expression levels of iNOS and COX-2 were determined by Western blot analysis. Histograms show densitometry analyses of relative iNOS, COX-2 expression levels normalized against tubulin.

6) exhibited stronger NO inhibition than the 25-OH cucurbitacin (**3**) ($IC_{50} \geq 30$ μM). Compared with cucurbitacin B (**4**) [$IC_{50} = 8.5$ μM], cucurbitacin E (**6**) [$IC_{50} = 25.4$ μM] has one more double bond ($\Delta^{1,2}$). This suggested that the appearance of double bond $\Delta^{1,2}$ negatively influenced the NO inhibitory activity of cucurbitacin B (**4**); moreover, the 25-acetoxy group may be the key active site for the anti-inflammatory action of cucurbitacin derivatives. However, further investigations of the anti-inflammatory effects of these cucurbitacin derivatives of their *in vivo* efficacy are necessary.

4. Conclusion

In conclusion, two previously undescribed sterols [trichosanhemiketal A, B, (**1–2**)], together with 13 known compounds, were obtained from *T. kirilowii* roots. Among them, compounds **4**, **5**, **6**, and **8** showed significant inhibitory activities on LPS induced NO production in RAW264.7 macrophages. In addition, cucurbitacin B (**4**) inhibited iNOS and COX-2 expression in a concentration-dependent manner. To the best of our knowledge, this is the first reported isolation of compounds with a 13,14-*seco*-13,14-epoxyporiferastanes (**1–2**) skeleton from the Cucurbitaceae family.

Acknowledgements

This research was supported by the National Research Foundation of Korea (NRF), funded by the Ministry of Education – Korea (NRF-2016R1D1A1B03930246). We are grateful to the Korea Basic Science Institute (KBSI) for mass spectrometric measurements.

Appendix A. Supplementary material

Supplementary data to this article can be found online at https://doi.org/10.1016/j.bioorg.2018.10.019.

References

[1] C. Jeffrey, Bot. J. Linn. Soc. 81 (1980) 233–247.
[2] M. Pitrat, M. Chauvet, C. Foury, I. Int. Symp. Cucurbits 492 (1997) 21–28.
[3] K. Pruesapan, R. Van Der Ham, Grana 44 (2005) 75–90.
[4] E.F. Fang, T.B. Ng, P.C. Shaw, R.N.S. Wong, Curr. Med. Chem. 18 (2011) 4410–4417.
[5] M. Khandaker, S. Akter, M.Z. Imam, Food Sci. Hum. Wellness. 7 (2018) 34–38.
[6] L. Da-Hui, J. Gui-Liang, Z. Ying-Tao, A. Tie-Min, Appl. Microbiol. Biotechnol. 74 (2007) 146–151.
[7] J.H. Choi, D.Y. Kim, J.H. Yoon, H.Y. Youn, J.B. Yi, H.I. Rhee, K.H. Ryu, K. Jung, C.K. Han, W.J. Kwak, Y.B. Cho, Osteoarthr. Cartil. 10 (2002) 471–478.
[8] T. Wu, X.M. Cheng, S.W. Bligh, G.X. Chou, Z.T. Wang, A. Bashall, C. Branford-White, Helv. Chim. Acta 88 (2005) 2617–2623.
[9] X. Chai, S.S. Li, L. Zhu, Y.F. Wang, X.M. Gao, Chem. Nat. Compd. 50 (2014) 965–967.
[10] N. Takahashi, Y. Yoshida, T. Sugiura, K. Matsuno, A. Fujino, U. Yamashita, Int. Immunopharmacol. 9 (2009) 508–513.
[11] Y. Xu, G. Chen, X. Lu, Z.Q. Li, S.S. Su, C. Zhou, Y.H. Pei, Biochem. Syst. Ecol. 43 (2012) 114–116.
[12] X.M. Fan, G. Chen, Y. Sha, X. Lu, M.X. Shen, H.M. Ma, Y.H. Pei, J. Asian Nat. Prod. Res. 14 (2012) 528–532.
[13] Y. Kimura, T. Akihisa, K. Yasukawa, M. Takido, T. Tamura, Chem. Pharm. Bull. 43 (1995) 1813–1817.
[14] T. Akihisa, H. Tokuda, E. Ichiishi, T. Mukainaka, M. Toriumi, M. Ukiya, K. Yasukawa, H. Nishino, Cancer Lett. 173 (2001) 9–14.
[15] P.C. Shaw, W.L. Chan, H.W. Yeung, T.B. Ng, Life Sci. 55 (1994) 253–262.
[16] M.T. Ha, S.H. Seong, T.D. Nguyen, W.-K. Cho, K.J. Ah, J.Y. Ma, M.H. Woo, J.S. Choi, B.S. Min, Phytochemistry. 155 (2018) 114–125.
[17] N.K. Im, Y.S. Jung, J.H. Choi, M.H. Yu, G.S. Jeong, Nat. Prod. Sci. 20 (2014) 51–57.
[18] N. Hai Dang, Y.-Y. Choo, N. Tien Dat, N. Hoai Nam, C. Van Minh, J.-H. Lee, J. Cell. Biochem. 117 (2016) 659–670.
[19] T. Kikuchi, Y. Horii, Y. Maekawa, Y. Masumoto, Y. In, K. Tomoo, H. Sato, A. Yamano, T. Yamada, R. Tanaka, J. Org. Chem. 82 (2017) 10611–10616.
[20] Z.X. Hu, Y.M. Shi, W.G. Wang, X.N. Li, X. Du, M. Liu, Y. Li, Y.B. Xue, Y.H. Zhang, J.X. Pu, H.D. Sun, Org. Lett. 17 (2015) 4616–4619.
[21] T. Itoh, Y. Kikuchi, T. Tamura, T. Matsumoto, Phytochemistry. 20 (1981) 761–764.
[22] T. Akihisa, Anal. Sterols Other Biol. Signif. Steroids (1989) 251–265.
[23] M.S. Bjelaković, L.B. Lorenc, V.D. Pavlović, B. Tinant, J.-P. Declercq, J. Kalvoda, Helv. Chim. Acta. 86 (2003) 2121–2135.
[24] C.-T. Che, X. Fang, C.H. Phoebe Jr, A.D. Kinghorn, N.R. Farnsworth, B. Yellin, S.M. Hecht, J. Nat. Prod. 48 (1985) 429–434.
[25] L. Yang, S. Wu, Q. Zhang, F. Liu, P. Wu, Cancer Lett. 256 (2007) 267–278.
[26] S. Kongtun, W. Jiratchariyakul, T. Kummalue, P. Tan-ariya, S. Kunnachak, A.W. Frahm, Planta Med. 75 (2009) 839–842.
[27] R.W. Doskotch, C.D. Hufford, Can. J. Chem. 48 (1970) 1787–1788.
[28] S.M. Kupchan, H. Meshulam, A.T. Sneden, Phytochemistry 17 (1978) 767–769.
[29] Y. Yamada, K. Hagiwara, K. Iguchi, S. Suzuki, H. Hsu, Chem. Pharm. Bull. 26 (1978) 3107–3112.
[30] A.G. González, J.A. Guillermo, A.G. Ravelo, I.A. Jimenez, M.P. Gupta, J. Nat. Prod. 57 (1994) 400–402.
[31] M.N. Galbraith, D.H.S. Horn, J. Chem. Soc. Chem. Commun. (1972) 113–114.
[32] X.W. Wang, H.P. Zhang, F. Chen, X. Wang, W.Y. Wen, Chin. Chem. Lett. 20 (2009) 589–591.
[33] C.L. Cantrell, B.P. Case, E.E. Mena, T.M. Kniffin, S.O. Duke, D.E. Wedge, J. Agric. Food Chem. 56 (2008) 5062–5068.